Development and Application of Analytical Strategies to Facilitate Protein-Ligand Binding Analysis on the Proteomic Scale

by

Dongyu Wang

Department of Chemistry
Duke University

Date:_____

Approved:

_____
Michael C. Fitzgerald, Supervisor

_____
Jie Liu

_____
Jiyong Hong

Thesis submitted in partial fulfillment of
the requirements for the degree of
Master of Science in the Department of
Chemistry in the Graduate School
of Duke University

2013

ABSTRACT

Development and Application of Analytical Strategies to Facilitate Protein-Ligand Binding Analysis on the Proteomic Scale

by

Dongyu Wang

Department of Chemistry
Duke University

Date:_____

Approved:

_____
Michael C. Fitzgerald, Supervisor

_____
Jie Liu

_____
Jiyong Hong

An abstract of a thesis submitted in partial fulfillment of the requirements for the degree of Master of Science in the Department of Chemistry in the Graduate School of Duke University

2013

Abstract

SPROX (Stability of Proteins from Rates of Oxidation) is a technique for the detection and quantitation of protein-ligand binding interactions. In SPROX the differential denaturant dependence of a methionine oxidation reaction in proteins performed in the presence and in the absence of ligand is used to measure the thermodynamic properties of protein-ligand binding interactions. Recently, the SPROX technique has also been used with quantitative mass spectrometry-based proteomic strategies to simultaneously assay up to hundreds of different proteins in complex biological samples. The proteomic applications of SPROX, to date, have relied on the use of a methionine-containing-peptide enhancement strategy and 1-D liquid chromatography–tandem mass spectrometry (LC-MS/MS) and. The strategies presented here, including gel electrophoresis fractionation and gas-phase fractionation of derivatized methionine-containing peptides, aim to increase proteomic coverage in SPROX by facilitating the detection, identification, and quantitation of methionine-containing peptides in the proteomics experiment. The initial results obtained in this work have shown that gel electrophoresis can help increase the proteome coverage while identifying complementary peptides to the current solution-based SPROX analysis. A gas-phase fractionation strategy is also demonstrated; however, the mass spectrometric analysis needs to be optimized and further tested to achieve selectivity for methionine peptides. Both of these fractionation strategies show promise for improving

the proteomic coverage in SPROX studies of protein-ligand interactions on the proteomic scale. In addition, the previously established SPROX protocol using isobaric mass tags was used in two protein-ligand binding experiments, including one experiment to identify the protein targets in a yeast cell lysate of adenosine 5′-(β,γ-imido)triphosphate (AMP-PNP), a non-hydrolyzable adenosine-5'-triphosphate (ATP) mimic, and second experiment to investigate the protein targets of two iron chelators, deferasirox (Exjade) and N'-[1-(2hydroxyphenyl) ethyliden]isonicotinoylhydrazide (HAPI), both of which protect ARPE-19 cells from oxidative damage induced by hydrogen peroxide. Three known ATP-binding proteins, ADEnine requiring, URAcil requiring and Yeast Elongation Factor, have been identified, while further investigation for the protein targets of iron chelators needs to be performed.

Dedication

I would like to express my deepest and sincerest appreciation to my advisor Prof. Michael C. Fitzgerald for his dedicated directions, countless encouragements and tremendous support over the past three years. Michael provided valuable suggestions to improve my research work as well as scientific writing and oral presentation. Actually, his guidance has helped me in every accomplishment I made. Moreover, I have sensed his great passion on science since I joined the group, which has inspired me to work hard and to enthuse about my research. The knowledge and experience I have obtained from him will certain affect profoundly my future career.

I want to sincerely thank my committee member Prof. Jie Liu. Not only has he committed his time and effort to help me with my studies, he has also contributed to offer treasured encouragements and support with my personal life in the U.S. I would also like to thank Prof. Jiyong Hong and Prof. Terry Oas, who have taken time for being my committee members and providing constructive comments and suggestions on my research. Without such help and support from the committee members, I would never have been able to finish my work.

Furthermore, I would love to show my gratitude to my family, especially my parents whose spiritual support is even more important. It is them who raised me with incredible care and love; it is them who taught me a great amount of philosophy of life; it is them whose dedication and sacrifice as well as understanding and encouragement

support me to go through all the difficulties and sufferings. Without these important and indispensable parts, my life would not have been so beautiful and colorful.

Finally, I would like to give my special thanks to all the past and current members of Fitzgerald's group, Ying, Patrick, Duc, Erin, Ariel, Jagat, Yingrong, Lorraine, Ryenne and Julia, for their helpful and insightful discussions, their thoughtful help and their memorable friendships. They create a harmonious and pleasant working environment and I feel very enjoyable working with them. I extend extra thanks to Yifei Wang who had helped me synthesize the heave phenacylbromide for my research work.

Contents

List of Tables

List of Figures

1. INTRODUCTION

The study of protein-ligand binding interactions in complex organisms is important for understanding cellular processes and drug mode-of-action. It provides important information related function and regulation of proteins and the roles of small molecules. The comprehensive analysis of proteome-wide protein-ligand interactions, specifically, requires the detection of all interactions and quantitation of binding affinities.

Current protein–ligand binding assays are insufficient to obtain such a comprehensive analysis in complex mixtures. Conventional protein–ligand binding techniques[1-4] (e.g., spectroscopic or calorimetric methods) require large amounts of highly purified protein. The yeast two-hybrid assay[5-8] and affinity-based[9-11] separation techniques coupled with mass spectrometry (MS) cannot provide quantitative information about protein–ligand interactions and are challenged by indirect interactions and interactions with small-molecule ligands. Several H/D exchange techniques coupled with MS[12-16] suffer the limitations from signal suppression issues and the resolving power of modern mass spectrometers and thus can only analyze relatively simple protein mixtures.

To help solve these problems, an MS-based technique for detection and quantitation of protein-ligand interactions on the proteomic scale has recently been developed at Duke University in the Fitzgerald lab[17-19]. This technique utilizes SPROX

incorporated with isobaric mass tags (i.e., iTRAQ, isobaric tag for relative and absolute quantitation) and a strategy to enrich the unoxidized methionine-containing peptides through chemo-selectively separation. SPROX can measure the stabilization or destabilization of the proteins caused by a ligand binding. The technique relies on the use of the denaturant dependence of oxidation of methionine (Met) side chains in proteins by hydrogen peroxide, both in the presence and absence of a ligand[17-19]. It has been demonstrated that such a bottom-up proteomics technique can make quantitative thermodynamic measurements of protein-ligand binding on the proteomic scale[17]. To date, approximately 500 peptides from approximately 350 proteins have been identified with 1D LC-MS/MS analysis[17].

However, the application of this technique is limited by several issues that ultimately impact the number of proteins identified in complex mixtures and the accuracy of the quantitative information. First, a data-dependent acquisition is used in the LC-MS/MS analysis step, which makes difficult the inclusion of low abundant proteins in the assay. Also, there are a number of steps involved in the protocol which require many sample manipulations that can lead to significant material losses. In addition, reliable quantitation is only achievable when samples are handled identically before labeling while many differential factors affect the identity of samples, such as TCA precipitation recovery and digestion efficiency. Thus, new approaches are needed

to increase proteomic coverage and Met selectivity as well as improve quantitation capabilities for studies in protein-ligand interactions.

1.1 Method Development

Described here are two such improved strategies. One involves gel electrophoresis and another involves the gas-phase fractionation of derivatized Met-containing peptides.

1.1.1 Gel Electrophoresis

Gel electrophoresis (GE) separates proteins in complex mixtures according to their size and as a consequence, reduces the complexity of samples and provides the prerequisite for a substantial proteome analysis using MS/MS[20-23]. Even though there are drawbacks, such as being labor intensive and limited in dynamic range of proteins, GE has proven to be a successful proteomic strategy when incorporated with MS.

1.1.2 Gas-phase Fractionation

The general principle of the phenacylbromide (PAB)-induced derivatization and the selective gas-phase fragmentation of Met-containing peptides is represented in Figure 1. The gas-phase fragmentation of the fixed-charge derivatives can lead to an exclusive neutral loss (CH_3SR) and characteristic cyclic six- (Pathway 1) and/or five-membered (Pathway 2) product ions, via S_N2 reactions involving either the C- and/or N-terminal amide carbonyl groups attacking the neighboring derivatized side chain[24-26]. Thus, the selection of Met-containing peptides from complex mixtures can be achieved

via neutral loss (NL) scanning method, without additional fractionation or enrichment[25, 27]. Identification of these peptides can be accomplished by energy resolved "pseudo MS^3" in a triple quadrupole mass spectrometer[25, 27]. Quantitation of proteins is possible by measuring the relative abundances of the NL product ions of the "light" and "heavy" isotopically labeled peptides[25, 27]. Accordingly, gas-phase fractionation of derivatized Met-containing peptides strategy is significant for identification and quantitation of Met-containing proteins with high sensitivity and selectivity.

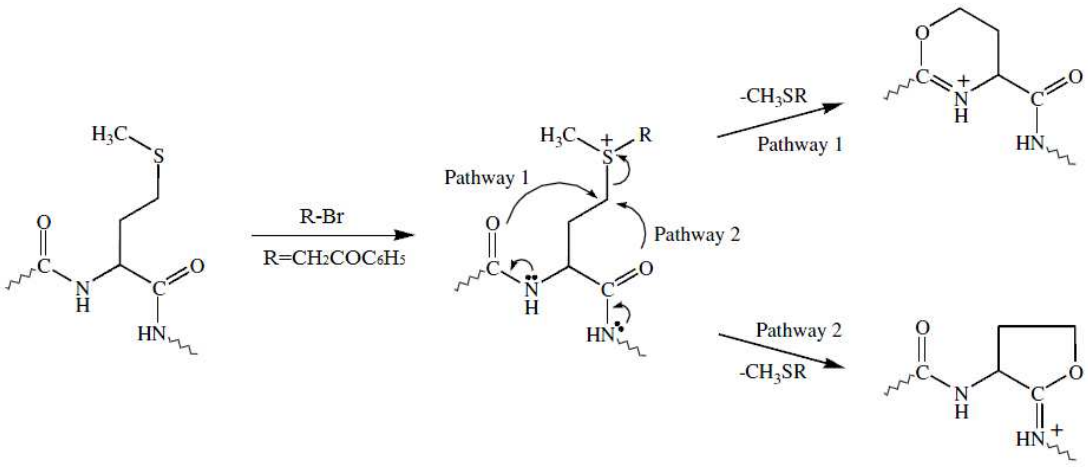

Figure 1: Fixed-charge side chain sulfonium ion derivatization and selective gas-phase fragmentation of methionine-containing peptides.

1.2 Method Application

1.2.1 Exploration of ATP-catalyzed Metabolism within Yeast Cells

ATP is a multifunctional nucleoside triphosphate: it is the energy source and can be used by enzymes and structural proteins in many metabolic processes; it can also

regulate many biochemical pathways[28-36]. Consequently, ATP plays an important role for metabolism within cells and the study of protein-ligand binding interactions of ATP will provide us important information of these metabolisms. AMP-PNP is a non-hydrolyzable ATP mimic. It competitively inhibits a number of metabolic reactions involved the hydrolysis of ATP[37] and thus is more suitable to be used in our study. The structures of ATP and AMP-PNP are shown in Figure 2.

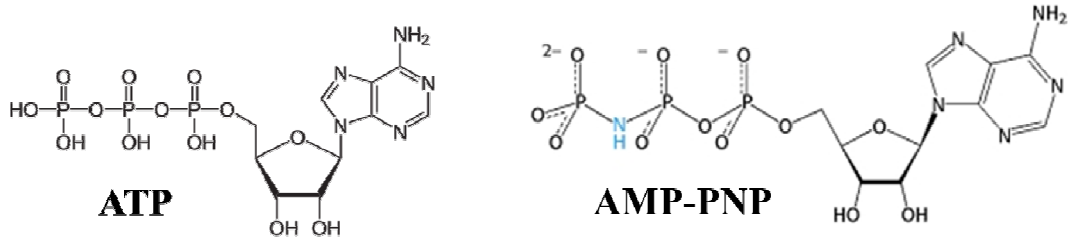

Figure 2: Structures of ATP and AMP-PNP

1.2.2 Identification of Iron Chelators Protecting Mechanism in Mammalian Cells

Iron plays an essential role in a wide range of physiological processes due to its ability to accept and donate electrons while redox cycling between the Fe^{2+} and Fe^{3+} oxidation states[38]; however, excess labile iron can also catalyze the formation of highly toxic hydroxyl radicals through the Fenton reaction. Iron chelation has been demonstrated as an effective therapy for disease states of iron overload[39, 40], which may be caused by routine blood transfusion required by patients with anemia[41]. Recent efforts are made to expand the application of iron chelating agents for treating other

diseases, such as cardiovascular disease, associated with localized iron-catalyzed oxidative stress instead of systemic iron overload[42-53]. Previous results suggest that different chelators exhibit different degree of cytotoxicity and distinct efficiency in protecting cells from oxidative stress[44] and among them, Exjade and HAPI (Figure 3) have shown potent cytoprotective effects[54-57]. The identification of their intracellular protein targets will help us better explore the underlying mechanisms and molecular basis of cytotoxicity and cytoprotection of these iron chelators.

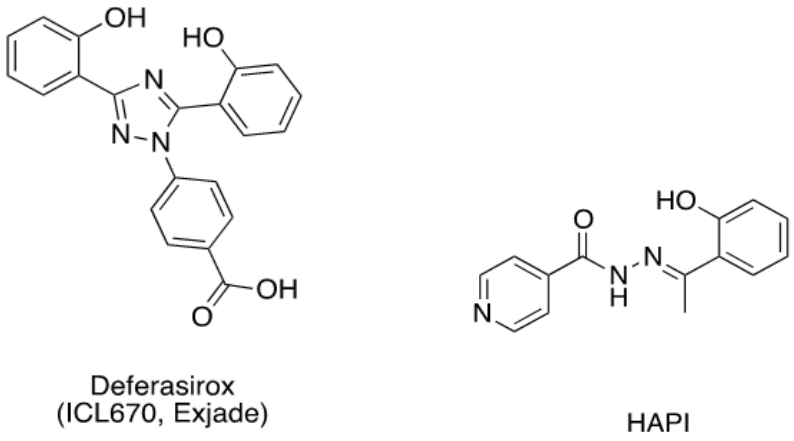

Figure 3: Structures of iron chelators Exjade and HAPI

2. EXPERIMENTAL SECTION

2.1 Cell Culture and Protein Sample Preparation

2.1.1 Yeast Cell Culture

A colony of Saccharomyces cerevisiae Y258 strain was inoculated in 10 mL of YPD media containing 1% yeast extract, 2% peptone, and 2% dextrose and incubated at 30 °C overnight. Then 2 mL of this endogenous yeast cell culture was added to 1 L of YPD media in a 2 L flask, growing at 30 °C, until the OD_{600} was 0.8-1.2. After centrifuging 250 mL portions of the cell culture at 2500 x g for 10 min at 4 °C, the supernatant was removed and each yeast cell pellet was resuspend with 1 mL of distilled water. The cell suspensions were then aliquoted to 1ml and pipetted into 2 mL plastic microcentrifuge tubes. The supernatant in each tube was removed after centrifuging at 5000 x g for 10 min at 4 °C. Yeast cell pellets were stored at -20 °C and thawed on ice prior to use. Cell pellets were lysed in 500μL 20mM phosphate buffer (pH=7.4) with 5 μL protease inhibitor and acid-washed glass beads. After vortexing on a Disruptor Genie 15 times for 20s each time with 1min on ice in between lyses, lysates were centrifuged at 15000 × g for 10min and the total protein concentration in the supernatant was measured using a Bradford assay.

2.1.2 Mammalian Cell Culture

The spontaneously immortalized human retinal pigment epithelial cell line ARPE-19 and cervical cancer cell line Hela were purchased from American Type Culture

Collection. ARPE-19 cells were grown in 1:1 Dulbecco's modified eagle medium (DMEM) and F12 Ham's nutrient mix (F12) medium supplemented with fetal bovine serum (FBS) (10%), pencillin–streptomycin (pen-strep) (1%), and L-glutamine (1%), while Hela cells were grown in DMEM supplemented with FBS (10%), pen-strep (1%). Cells were initially cultured in 75cm^2 tissue culture flasks until confluent. The growth medium was removed and cell layer was briefly rinsed with 10 mL phosphate (PBS) buffer. The flasks were kept in the incubator at 37°C after added 2 mL of 0.25% (w/v) Trypsin- 0.53 mM EDTA solution, and 8 mL of growth medium was then added to the flask when cell layer was dispersed. Cells were aspirated by gently pipetting and 2 mL aliquots of the cell suspension were added to new 15 cm petri dishes. After cells were confluent, the growth media were removed and cells were washed twice with ice-cold PBS buffer before scraped from the dishes. Mammalian cell pellets were then collected in 300 μL PBS buffer containing 1% Halt Protease and Phosphatase Inhibitor Cocktail and lysed with bigger acid-washed glass beads (diameter≈1mm). After vortexing 20 times for 20s each time with 1min on ice in between lyses, lysates were centrifuged at 15000 × g for 10min and the total protein concentration in the supernatant was measured using a Bradford assay.

2.2 SPROX Protocol using Isobaric Mass Tags

The SPROX protocol used in this work is essentially identical to that previously described[58]. The specific experimental details about the use of this protocol in this work are given below.

2.2.1 SPROX with Isobaric Mass Tags Protocol

Figure 4 shows the schematic of the SPROX protocol with isobaric mass tags (SPROX-iTRAQ). Each lysate sample (X amount of protein in 20 μL) was added to a series of SPROX buffers (25 μL) with increasing denaturant concentration, and then oxidized by 5 μL of 9.8 M (30% w/w) H_2O_2 after equilibration of the protein samples in the SPROX buffers for 30min. After 3 min, oxidation was quenched with 1 mL of a 300 mM methionine solution followed by adding 200 μL 1 g/mL ice-cold trichloroacetic acid (TCA) to precipitate proteins overnight. Samples were centrifuged at 8000 × g for 30min at 4°C and the pellets were washed with 300 μL ice-cold ethanol three times. After removing all residual ethanol by a SpeedVac concentrator, samples were redissolved in 30μL 0.5M triethylammonium bicarbonate (TEAB) buffer (pH=8.5) with 0.1% sodium dodecyl sulfate (SDS) and vortexed for 1h. Sample concentration after redissolving was determined by Bradford assay. According to manufacturer's protocol of iTRAQ's reagent, disulfide bonds were reduced in 5 mM tris-(2-carboxyethyl) phosphine hydrochloride (TCEP·HCl) and cysteine residues were alkylated by 10 mM S-methyl methanethiosulfonate (MMTS). Then samples were digested with trypsin at 37°C

overnight (E:P=1:50, w/w) and labeled with 0.5 units of corresponding iTRAQ in 50 μL isopropyl alcohol for 2h at room temperature. Samples were combined and desalted using C_{18} resin and/or Pi^3-Met resin (The Nest Group) according to the manufacturer's protocol or and eluted with 25 mM formic acid (FA) in 70% acetonitrile (ACN). Samples were subjected to LC-MS/MS analysis after ACN was removed using the SpeedVac concentrator and 0.1% FA (300 μL) was added.

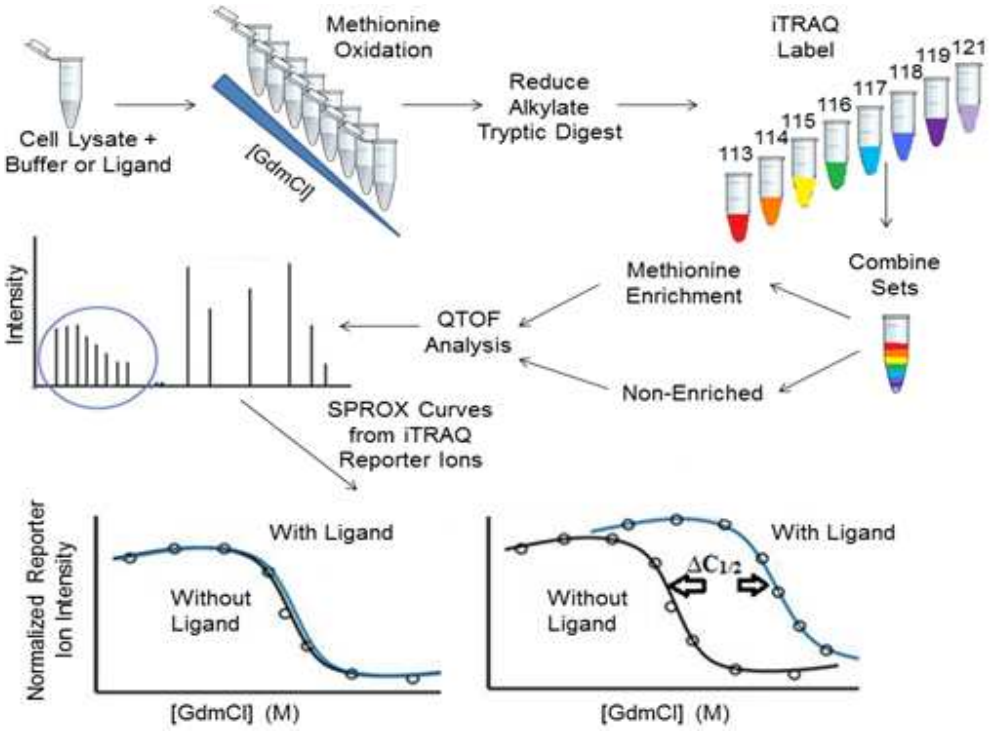

Figure 4: Schematic of Standard SPROX-iTRAQ Protocol

2.2.2 Quantitative Proteomic Sample Analysis with ESI-Qq-TOF

Samples were analyzed on an Agilent 6520 Q-TOF mass spectrometer system, equipped with a Chip Cube Interface and an enrichment column consisted of 150mm ×

75μm Zorbax 300SB-C18 5μm packing. Buffer A was 0.1% FA in water and Buffer B was 0.1% FA in ACN. With a 116min elution linear gradient, increasing percentage of Buffer B was used from 5% to 100%, with a flow rate of 0.4 μL/min: samples were eluted with 5% to 15% Buffer B for 7.5min, 15% to 45%Buffer B for 78min, 45% to 100% Buffer B for 20min, and then 5% Buffer B for 10.5min. Other parameters are shown in Table 1. Samples were analyzed in a data dependent acquisition and four precursor ions were selected for fragmentation per cycle.

Table 1: Parameters used for quantitative proteomic sample analysis with ESI-Qq-TOF.

Drying Gas Flow Rate	Skimme	Fragmentor	Capillary Voltage
6L/min (350oC)	65V	175V	1850V
Collision Energy (Typically for Sequencing)	Inclusion Window Width for Precursors	Scan Rate for Precursors	Scan Rate for Products
3.5V/100Da	4 m/z	3 scans/second	2 scans/second

2.2.3 Quantitative Proteomic Data Analysis

2.2.3.1 Search parameter for Spectrum Mill software

Agilent's Spectrum Mill MS Proteomics Workbench software was used for quantitative proteomic data analysis. Search parameters included Carbamidomethylation or cysteines alkylation with MMTS as a fixed modification on C-terminus, no modification or iTRAQ 8-plex reagent labeling as a fixed modification on N-terminus, deamidation of glutamines and asparagines, and oxidation of methionines

as variable modifications. The mass tolerances of precursor and product ions were set to 20ppm, the protein cleavage chemistry was set for trypsin with 3 maximum missed cleavages, and the maximum ambiguous precursor charge was set to 7. Searches were against the NCBInr database for S. cerevisiae. False positive rate was determined by searching against the entire S. cerevisiae database of reversed protein sequences with the same search parameters. With iTRAQ, the labeling efficiency can be monitored by searching the product ion mass spectrum of the labeled peptides againest the NCBInr database for S. cerevisiae with the iTRAQ as a variable modification on N-terminus. Thus, the number of non-labeled peptides was also displayed and the labeling efficiency can be determined by the equation: Labeling efficiency=the number of labeled peptides / (the number of labeled peptides + the number of non-labeled peptides).

2.2.3.2. SPROX data analysis

The iTRAQ intensities of identified peptides were extracted by Spectrum Mill; however, only the fragment ions with adequate iTRAQ intensities, that is, raw reporter ion intensities should be larger than 125 count per reporter ion averagely, were used for quantitation. The raw intensity of each iTRAQ tag was firstly divided by the average of all the iTRAQ intensities for a particular peptide to generate the first normalization factor (N1), and the N1 for the Met peptides were then divided by the average of the N1 for all the non-Met peptides to generate the second normalization factor (N2) for the Met peptides, that is the normalized reporter ion intensities in the SPROX data sets. The Met

peptides that are common to both the with and without ligand samples were determined with the program. The distribution at the low denaturant concentration for the unoxidized Met peptides has the maximum normalized reporter ion intensity, which is the pre-transition baseline of SPROX data set, while the distribution at the high denaturant concentration for the unoxidized Met peptides has the minimum normalized intensity, which is the post-transition baseline. The normalized reporter ion intensity for maximum separation between the pre- and post-transition baselines in the SPROX data was named the "cut-off" value and determined by the distributions of the normalized intensities at the highest and lowest denaturant concentrations. Accordingly, transition midpoints were assigned by visual inspection of the normalized intensities.

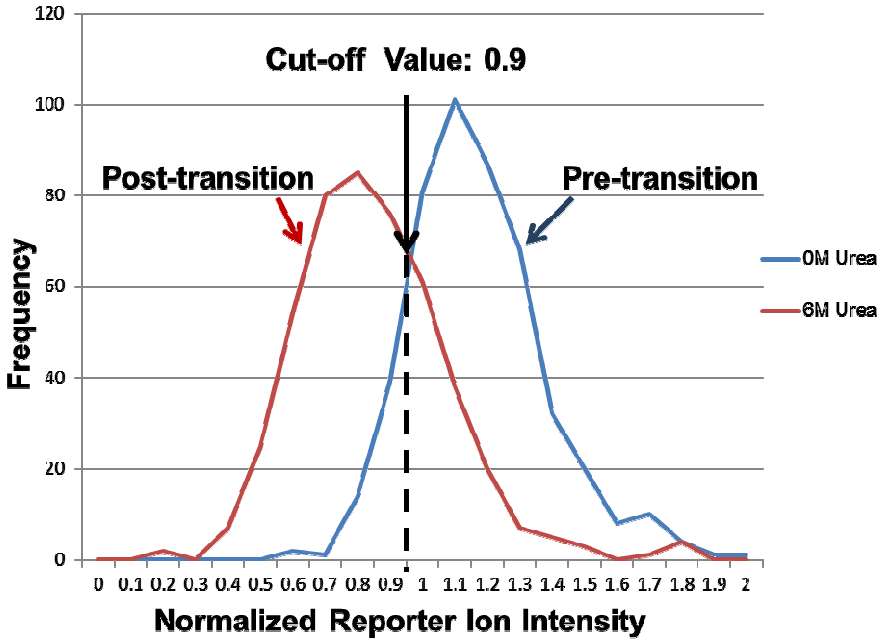

Figure 5: Distribution of normalized reporter ion intensities for unoxidized Met peptides of 0M and 6M urea samples in the ATP-binding experiment. The

distribution gives an indication of what an ideal SPROX curve should look like. The point of maximum separation where the two distributions intersect is called the cut-off value, and its location is denoted with an arrow.

Figure 5 shows the distribution of normalized reporter ion intensities for unoxidized Met peptides of 0 M urea and 6 M urea samples in the ATP-binding experiment. The 0M urea distribution has maximum intensity at a normalized reporter ion intensity of 1.1, which is deemed pre-transition. The 6M urea distribution has a maximum normalized reporter ion intensity of 0.7, which is referred to as post-transition. The point of maximum separation between 0M and 6M urea is 0.9, which is the "cut-off" value. Therefore, the SPROX data set for an unoxidized Met peptide should have a $C^{1/2}_{SPROX}$ value at a normalized intensity of 0.9 (Figure 6).

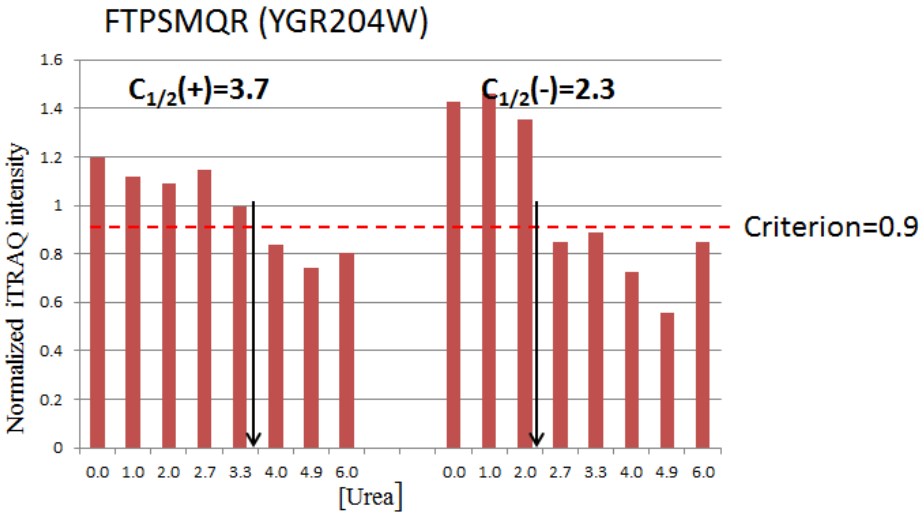

Figure 6: SPROX data of unoxidized Met peptide FTPSMQR from protein ADEnine requiring (YGR204W) in the ATP-binding experiment. The $C^{1/2}_{SPROX}$ values are indicated with an arrow, which are 3.7M urea for the with ligand sample and 2.3M urea for the without ligand sample.

2.3 Gel-phase Fractionation Interfaced with SPROX Experiment

2.3.1 iTRAQ-labeling Intact Protein Followed by In-gel Digestion Strategy

After SPROX analysis and TCA precipitation, samples were redissolved in 0.5 M 4-(2-Hydroxyethyl)-1-piperazinepropanesulfonic acid (EPPS) and 6 M urea buffer and vortexed for 1h. According to manufacturer's protocol of iTRAQ's reagent, disulfide bonds were reduced in 5 mM TCEP·HCl and cysteine residues were alkylated by 10 mM MMTS. Then samples were labeled with 0.5 units of corresponding iTRAQ in 50 μL isopropyl alcohol for 2h at room temperature and the labeling reaction was quenched by the addition of 10 mM lysine solution. Subsequently, samples were combined and loaded on a Tris-HCl 4–20% precast linear gradient polyacrylamide gel followed by staining with Coomassie Brilliant Blue R-250. Entire gel lanes were excised into pieces of 1 × 1mm and the gel pieces were transferred into 1.5 mL Eppendorf tubes. 50 mM ammonium bicarbonate (AmBic) with 50% ACN solution was used to wash the gel pieces for 10 min three times followed by dehydration in 100% ACN. After removing all residual ACN by the SpeedVac concentrator, the gel pieces were rehydrated with 25 mM AmBic containing chymotrypsin/Arg-C/Glu-C (E:P=1:20, w/w) on ice for 90min. Then digestion of proteins was performed overnight at 37°C and peptides were extracted twice with 50%ACN containing 5% FA. After directly combined, the extracts were desalted using C_{18} resin according to the manufacturer's protocol and acidified by addition of 0.1% FA to a final volume of 300 μL for LC-MS/MS analysis.

2.3.2 iTRAQ-labeling In-gel Digested Proteins Strategy

After SPROX analysis and TCA precipitation, samples were redissolved with 30 μL 5% β-mercaptoethanol in 1× SDS loading buffer containing 375 mM Tris-HCl (pH=6.8), 6% SDS, 50% Glycerol and 0.045% Bromophenol and vortexed for 1h. Subsequently, samples were loaded on a Tris-HCl 4–20% precast linear gradient polyacrylamide gel followed by staining. Entire gel lanes were excised into pieces and washed with 0.5 M TEAB buffer for 10min three times followed by dehydration in 100% ACN. After removing all residual ACN by the SpeedVac concentrator, disulfide bonds were reduced in 5 mM TCEP·HCl and cysteine residues were alkylated with 10 mM MMTS. Then samples were dehydrated with 100% ACN again and rehydrated with 0.5 M TEAB containing trypsin (E:P=1:20, w/w) on ice for 90min, after removing all residual ACN. Then digestion of proteins was performed overnight at 37°C and peptides were extracted twice with 50% ACN containing 5% FA. After directly combined, the extracts were completely dried with SpeedVac concentrator and redissolved in 0.5 M TEAB buffer. The iTRAQ-labeling was performed with 0.5 units of corresponding iTRAQ in 50 μL isopropyl alcohol for 2h at room temperature. Samples were desalted using C_{18} resin and subjected to LC-MS/MS analysis after ACN was removed using the SpeedVac concentrator and 0.1% FA (300 μL) was added.

2.4 Gas-phase Fractionation Interfaced with SPROX Experiment

2.4.1 "Heavy" Phenacyl-bromide Synthesis Protocol

$^{13}C_6$ Phenacyl-bromide (PAB) ($BrCH_2CO^{13}C_6H_5$) was synthesized according to the the following procedure. Initially, anhydrous AlCl3 (11.8 g, 89.3 mmol) was added in small portions to a stirred solution of $^{13}C_6$-Benzene (500 mg, 6.0 mmol) and bromoacetyl bromide (646 L, 7.4 mmol) in CS_2 (60 mL). The reaction was refluxed for 30min at 45°C and then cooled to room temperature. The product was carefully poured onto ice, extracted into dichloromethane (75 mL, 25 mL once and three times) and washed with water (45 mL, 15 mL once and three times). The organic layer was extracted and dried over anhydrous $MgSO_4$. It was then filtered and evaporated under reduced pressure to give the product $^{13}C_6$ PAB ($BrCH_2CO^{13}C_6H_5$) as light yellow solid. After NMR and GC-MS analysis, the product was confirmed as a highly purified compound.

2.4.2 Model Peptide and Protein Sample Preparation

100 μg Substance P (SubP) or Glucagon was dissolved in 100 μL of aqueous 20% HOAc with 30% ACN. The derivatization reaction was initialized by adding 10 μL 1 M solution of PAB or $^{13}C_6$-PAB freshly prepared in ACN. All derivatization reactions were allowed to proceed for 24h at room temperature and the "light" and "heavy" labeled samples were then pooled together.

10 μL 1 mM Ribonuclease A (RNaseA) was prepared in 90 μL 100 mM AmBic containing 0.1% Rapigest and heated at 40°C while shaking for 10min. Disulfide bonds

were reduced by 11.1 μL 100 mM dithiothreitol (DTT) at 80°C for 15min and cysteine residues were alkylated by 12.3 μL 200 mM iodoacetamide (IDA) at room temperature for 30 min in darkness. Immobilized trypsin was added (E:P=1:10, w/w) to digest RNaseA at 37°C for 1h followed by centrifuging at 10000 × g for 2min. Supernatant was collected and immobilized chymotrypsin was added (E:P=1:10, w/w) to the tryptic RNaseA at 37°C for 1h followed by centrifuging at 10000 × g for 2min. Supernatant was collected followed by addition of 80 μL HOAc and 120 μL ACN. The RNaseA sample was then divided into two identical samples and the derivatization reaction of each sample was initialized by adding 10 μL 1 M solution of PAB or $^{13}C_6$-PAB freshly prepared in ACN. After 24h, the "light" and "heavy" labeled samples were then pooled together.

2.4.3 Yeast Lysate Sample Preparation

Endogenous yeast pellets were lysed to obtain a yeast cell lysate with concentration of 50μg/μl. The lysate sample (4 μL) was added to 36 μL 100mM AmBic containing 0.1% Rapigest and heated at 40°C while shaking for 10min followed by reduction by 4.44 μL 100 mM DTT at 80°C for 15min and alkylation by 4.94 μL 200 mM IDA at room temperature for 30 min in darkness. The lysate sample was digested with trypsin (E:P=1:50, w/w) at 37°C overnight. After adding 40 μL HOAc and 60 μL ACN, the lysate sample was then divided into two identical samples. The derivatization reaction of each sample was initialized by adding 10 μL 1M solution of PAB or $^{13}C_6$-PAB

freshly prepared in ACN. After 24h, the "light" and "heavy" labeled samples were pooled together.

2.4.4 Instumentation

MALDI analysis was performed when derivatization reactions were initiated and completed after 24h. α-Cyano-4-hydroxycinnamic acid (HCCA) was used as the matrix (M:P=9:1,v/v) and the laser power was 35%. All samples for LC-MS/MS analysis were desalted using C_{18} resin and ended up with a volume of 300 μL by addition of 0.1% FA. Parameters used for quantitative proteomic sample analysis with ESI-Qq-TOF were described above in Section 2.2.2, except that different collision energy setting was used for gas-phase fractionation studies. For SubP samples, increasing collision energy settings for Collision-Induced Dissociation (CID) were used, which were 0.9V/100Da, 1.2V/100Da, 1.5V/100Da, 2.0V/100Da, 2.5V/100Da, 2.7V/100Da, 3.0V/100Da, 3.3V/100Da, 3.5V/100Da, 4.5V/100Da and 5.5V/100Da. For RNaseA and lysate samples, collision energy was set to 2.0V/100Da.

2.5 Exploration of ATP-catalyzed Metabolism within Yeast Cells

Initially, 20 μL of 100 mM $MgCl_2$ was added to 160 μL aliquots of the yeast cell lysate, 20 μL of 200 mM AMP-PNP was added to one yeast cell lysate and 20 μL of lysis buffer was added to the other lysate in order to generate the with ligand (+) and without ligand (-) samples, respectively, and 20 μL aliquot of each sample were combined with 75 μL of each denaturant-containing buffer stock solution, which was prepared in 0.1 M

Tris buffer (pH=7.4) with urea concentrations that ranged from 0 to 8 M. The final urea concentration in the eight denaturant-containing buffers used for the ATP binding experiment were 0, 1, 2, 2.7, 3.3, 4, 4.8, and 6 M. The samples were dealt with standard SPROX with isobaric mass tags protocol (*See Section 2.2.1*). LC-MS/MS analysis was performed using an LTQ Orbitrap mass spectrometer (Thermo-Scientific, Inc). The non-enhanced (-) and (+) ligand samples and Met-enhanced (-) and (+) ligand samples were then subjected into the LC-MS/MS analysis, one run for each sample. SPROX data analysis process was described in Section 2.2.3.2.

2.6 Identification of Iron Chelators Protecting Mechanism in Mammalian Cells

The initial concentration of protein is 10μg/μL and of each ligand is 10 mM. The final GdmCl concentrations in the eight denaturant-containing buffers used for this experiment were 0.5, 1.0, 1.3, 1.7, 2.0, 2.5, 3.0 M and 3.5 M. The samples were dealt with standard SPROX with isobaric mass tags protocol (*See Section 2.2.1*). LC-MS/MS analysis was performed using an Agilent 6520 Q-TOF mass spectrometer system *(See Section 2.2.2).* The non-enhanced with and without ligand samples were then subjected into the LC-MS/MS analysis, three runs for each sample. Search parameter for Spectrum Mill software and SPROX data analysis process were described above in Section 2.2.3.

3. RESULTS AND DISCUSSION FOR METHOD DEVELOPMENT

3.1 Gel-Phase Fractionation Experiment

In the gel-phase fractionation experiment, the research goal was to employ GE to increase the proteome coverage and to determine the quantitation capabilities of this strategy for studies in protein-ligand interactions.

3.1.1 Verification of Whether Gel Electrophoresis Could Help Increase Proteome Coverage

A test experiment to determine whether in-gel digestion could help increase proteome coverage was initially performed on a yeast cell lysate. After resolution of proteins by GE, each entire lane of the gel was excised into two bands and proteins within the gel were digested with trypsin. The verification was carried out via comparing the results of in-gel digestion and in-solution digestion. More peptides (729 peptides in-gel vs. 389 peptides in-solution) were identified with the GE strategy and there was small partial overlap (38 peptides) between the results of in-gel digestion and in-solution digestion. These results substantiate that GE can help obtain complementary peptide identification to those of solution-phase technique and accordingly, indeed increase the proteome coverage.

3.1.2 Validation of The Strategy of iTRAQ-labeling In-gel Digested Proteins

A SPROX analysis was performed on a yeast cell lysate. After resolution of proteins by GE, entire lanes were excised into pieces and proteins within the gel were digested with trypsin. Then the resulting peptides were labeled with iTRAQ 6-plex reagent. The experiment was performed in duplicate. A comparison of the results obtained in duplicate experiments is shown in Table 2. When score threshold was set to 6, among 79 peptides identified in trial one and 93 peptides identified in trial two, 69 peptides were the same. Such a substantial overlap of peptide identification with consistent and low false positive rate shows the satisfying reproducibility of iTRAQ-labeling in-gel digested proteins for peptide identification.

Table 2: Comparison between the results of duplicate experiments for iTRAQ-labeling in-gel digested proteins strategy. The false discovery rates of the duplicate experiments were both less than 10% when the score was set to greater than 6.

Score>6	*Peptide (Unique)*	*Protein (Unique)*
Trial One	79	52
Trial Two	93	56
Overlap	69	39

The result of trial two was further analyzed. Among 93 unique peptides from 56 proteins, 55 unique peptides from 46 proteins had adequate iTRAQ intensity for quantitation (total iTRAQ intensity was larger than 750). Among them, 11 peptides from 11 proteins were Met-containing peptides; 44 peptides from 38 proteins were non-Met peptides; 7 peptides from 7 proteins were oxidized Met peptides; and 5 peptides from 5

proteins were unoxidized Met peptides. Among the seven oxidized Met peptides, three have been identified and have the SPROX curves in our previous work[19]. The transition midpoints of peptides in these experiments were compared with those in the reference (Figure 7). The midpoints of each oxidized Met peptide identified with this strategy and in the reference are correspond with each other, respectively, which indicates the strategy of iTRAQ-labeling in-gel digested proteins can be employed for quantitation.

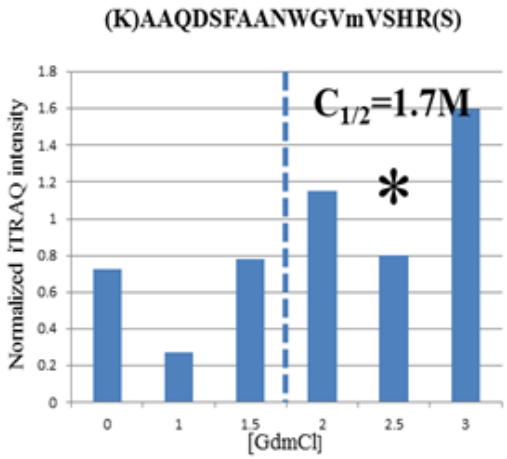

A1

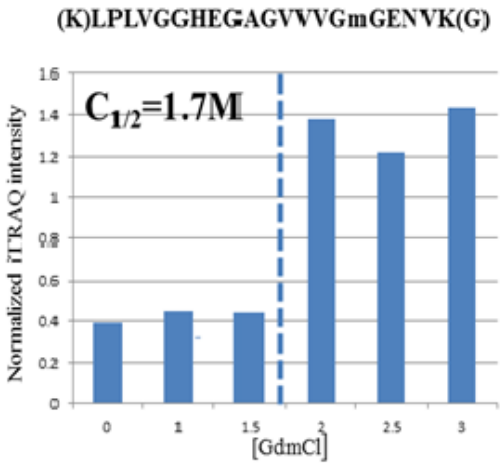

B1

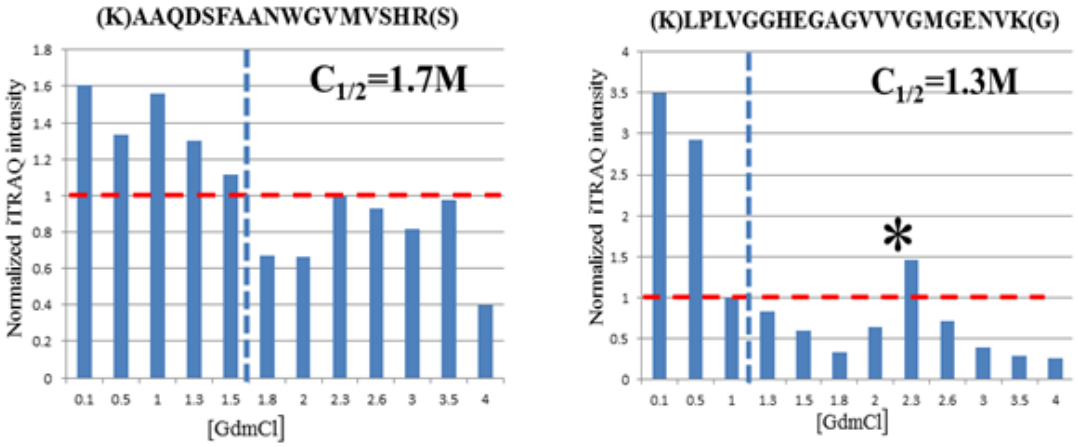

A2 B2

Figure 7: SPROX data of two Met peptides. The top ones are SPROX data of oxidized Met peptides identified in this experiment, while the bottom ones are SPROX data of unoxidized Met peptides identified in the reference[19]. (A1) SPROX data obtained on the AAQDSFAANWGVmVSHR peptide, the experimental midpoint is 1.7, which is 1.7 in the reference (shown in A2); (B) SPROX data obtained on the LPLVGGHEGAGVVVGmGENVK peptide, the experimental midpoint is 1.7, which is 1.3 in the reference (shown in B2). The GdmCl concentrations of the data sets in this experiment were (from left to right) 0, 1.0, 1.5, 2.0, 2.5, 3.0M, while they were (from left to right) 0.1, 0.5, 1.0, 1.3, 1.5, 1.8, 2.0, 2.3, 2.6, 3.0, 3.5, 4.0M in the reference. An asterisk represents an outlying data point.

3.2 Gas-Phase Fractionation Experiment

3.2.1 MALDI-TOF Results and LC-MS/MS Results of Substance P

SubP was dissolved in aqueous containing HOAc and ACN, and modified with 1M PAB directly. MALDI analysis was performed when reaction was initiated and 24h later (Figure 8). For modified SubP, the peak at m/z=1470.5 can be distinguished as the modified peak, since it is 119.0 away from the wild-type peak at m/z=1351.5. The peak at m/z=1304.4 can also be distinguished as the NL peak, since it is 166.1 away from the modified peak and -47.1 away from the wild-type peak. These results indicate that the

wild-type peak, the modified peak, and the NL peak can all be distinguished for SubP in the MALDI readouts.

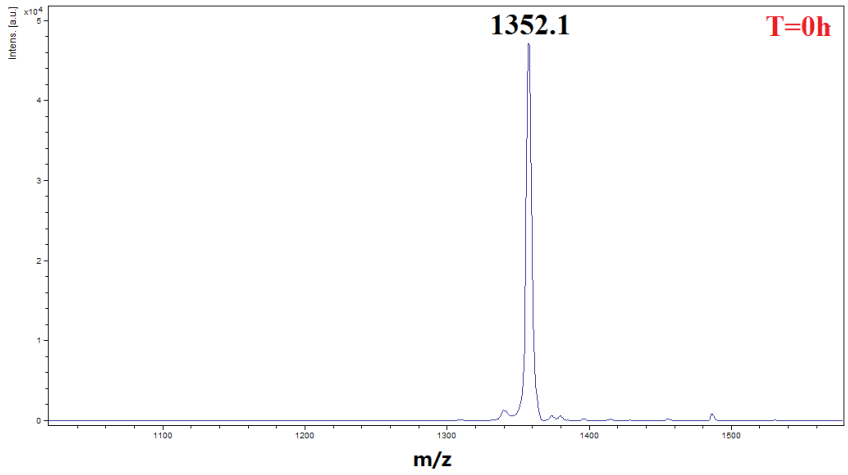

A

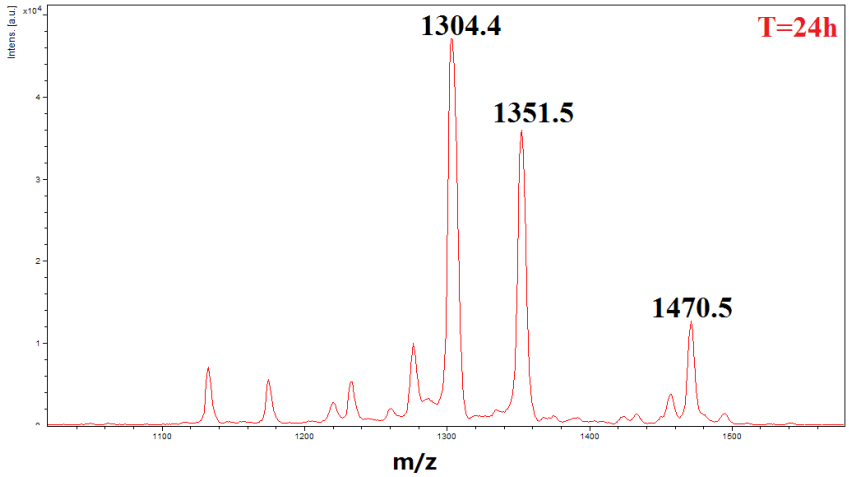

B

Figure 8: MALDI results of SubP. (A) The MALDI result of SubP 0h after modification. (B) The MALDI result of SubP 24h after modification.

SubP was then desalted using C_{18} column for LC-MS/MS analysis. Increasing collision energy was used for CID (Figure 9 and Figure 10).

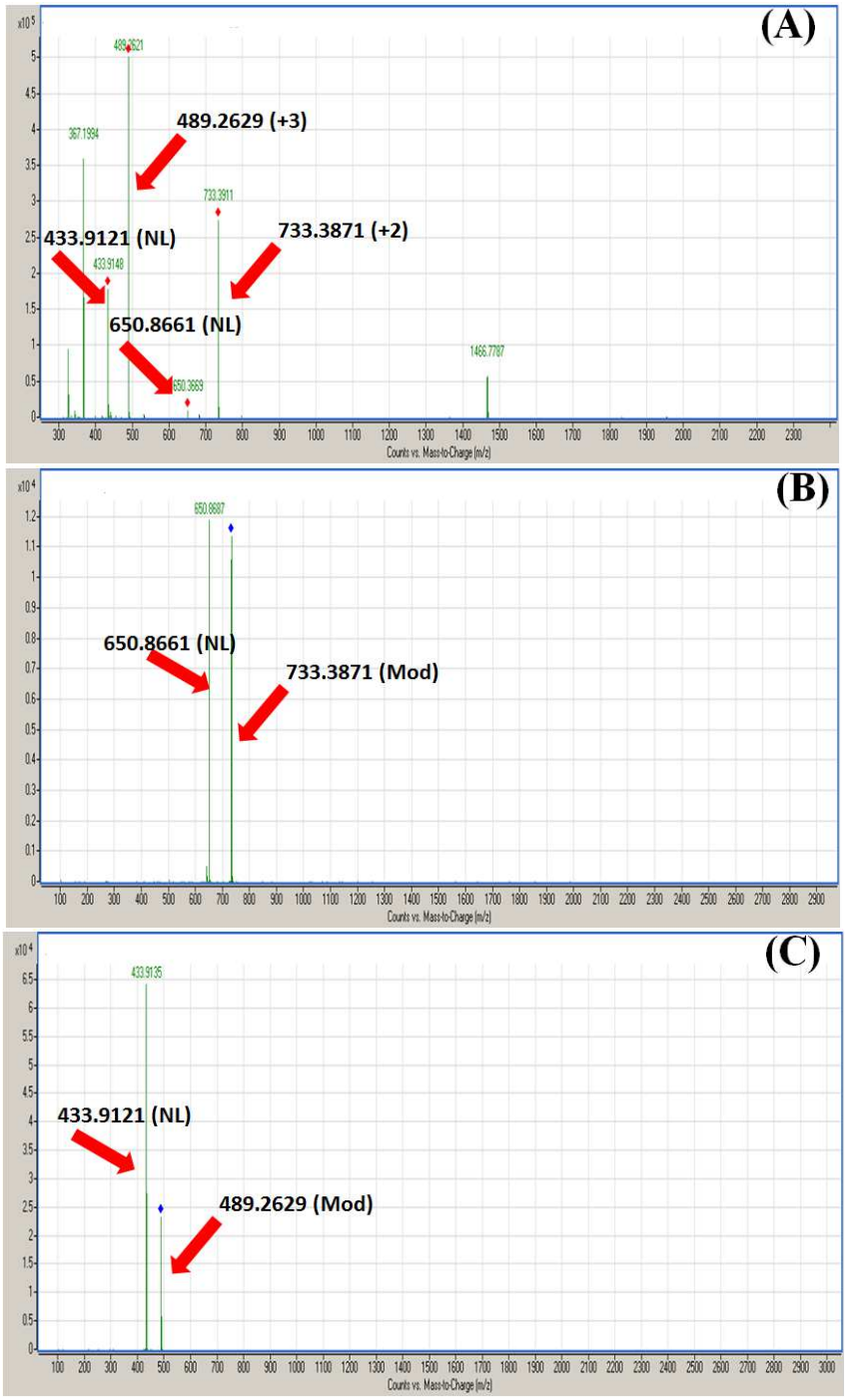

Figure 9: LC-MS/MS results of SubP when the collision energy was set at 2.0V/100Da. (A) Mass spectrum. (B) Product ion mass spectrum of doubly-charged ion at m/z=733.3871. (C) Produce ion mass spectrum of triply-charged ion at m/z=489.2629.

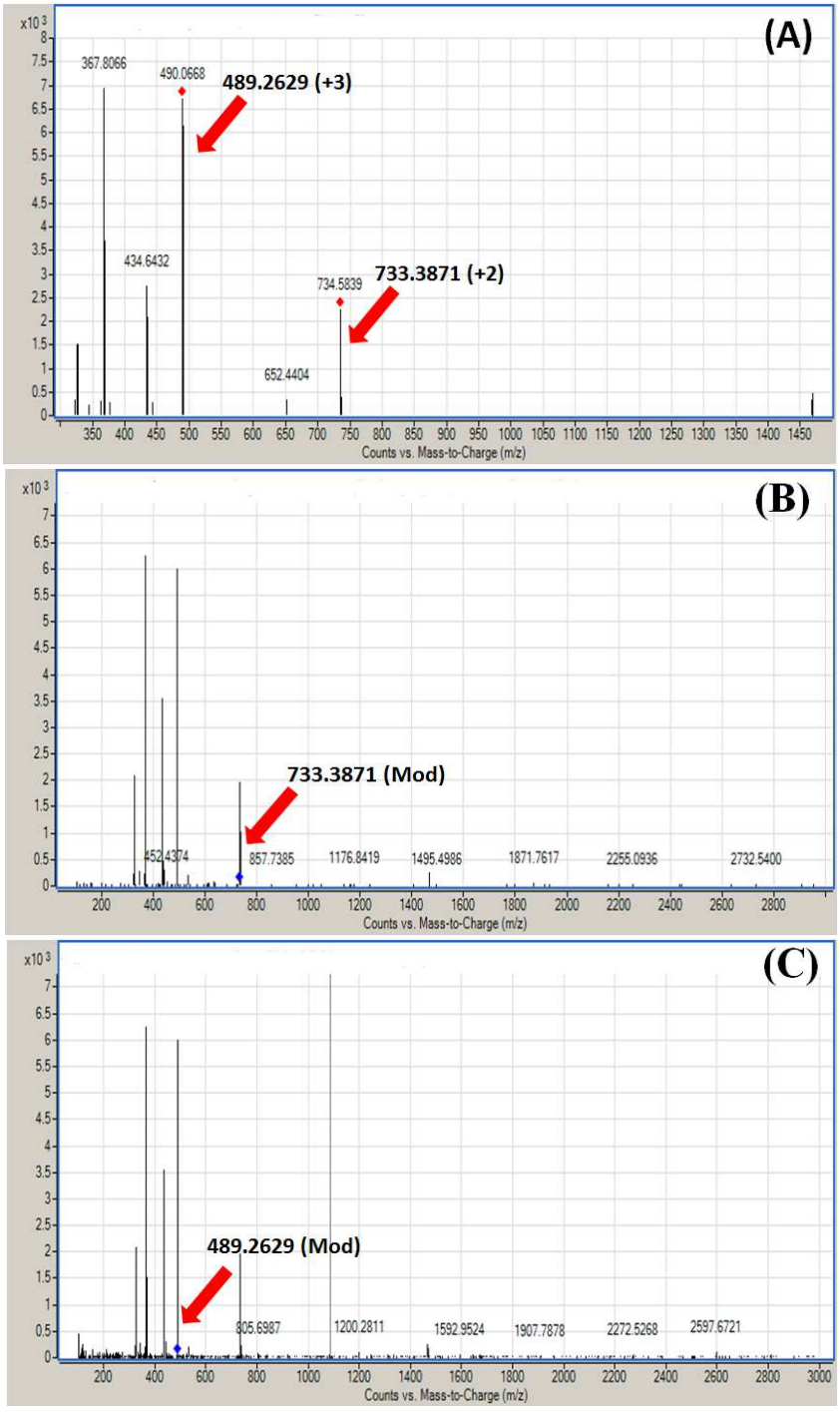

Figure 10: LC-MS/MS results of SubP when the collision energy was set at 4.5V/100Da. (A) Mass spectrum. (B) Product ion mass spectrum of doubly-charged ion at m/z=733.3871. (C) Product ion mass spectrum of triply-charged ion at m/z=489.2629.

The m/z of doubly-charged modified SubP is 733.3871 while the m/z of doubly-charged modified SubP with NL is 650.8661. The m/z of triply-charged modified SubP is 489.2629 while the m/z of triply-charged modified SubP with NL is 433.9121. In Figure 9, when the collision energy was set to 2.0V/100Da (which is about one half of the collision energy setting, 3.5V/100Da, that is typically used for sequencing), the modified peak and NL peak can be distinguished in both mass spectrum and product ion mass spectrum, and SubP itself hasn't been fragmented. The existence of the NL peak in mass spectrum may be because ESI conditions are such that the NL is occurring right from the source. The NL peak in product ion mass spectrum definitely came from the loss of $C_9H_{10}SO$ from the modified SubP. With increasing collision energy, the intensity ratio of NL peak and modified peak increased (data not shown) until the collision energy was set to 4.5V/100Da (which is about one and a third times of the collision energy setting typically used for sequencing). At that point, SubP was fragmented though the NL peak could still be distinguished with much lower intensity (Figure 10). Accordingly, low collision energy should be used on ESI-Qq-TOF for peptide/protein producing NL with high intensity.

3.2.2 LC-MS/MS Results of Peptide QHMDSSTSAASSSNY (QY) of "Light" Isotopically Labeled Ribonuclease A.

For peptide QY of modified RNaseA, similar results with SubP were achieved (Figure 11). When the collision energy was set at 2.0V/100Da (which is about one half of the collision energy setting, 3.5V/100Da, that is typically used for sequencing), the wild-

type peak was not seen; however, the modified peak and the NL peak can be seen in both mass spectrum and product ion mass spectrum and the peptide itself hasn't been fragmented. The m/z of triply-charged wild-type QY peptide is 524.8761, the m/z of triply-charged modified QY peptide is 564.2231 and the m/z of triply-charged modified QY peptide with NL is 509.2084. With increasing collision energy, the intensity ratio of the NL peak and the modified peak increased until the collision energy was set at 3.5V/100Da, the typical collision energy used for sequencing. At that point, the peptide QY was fragmented.

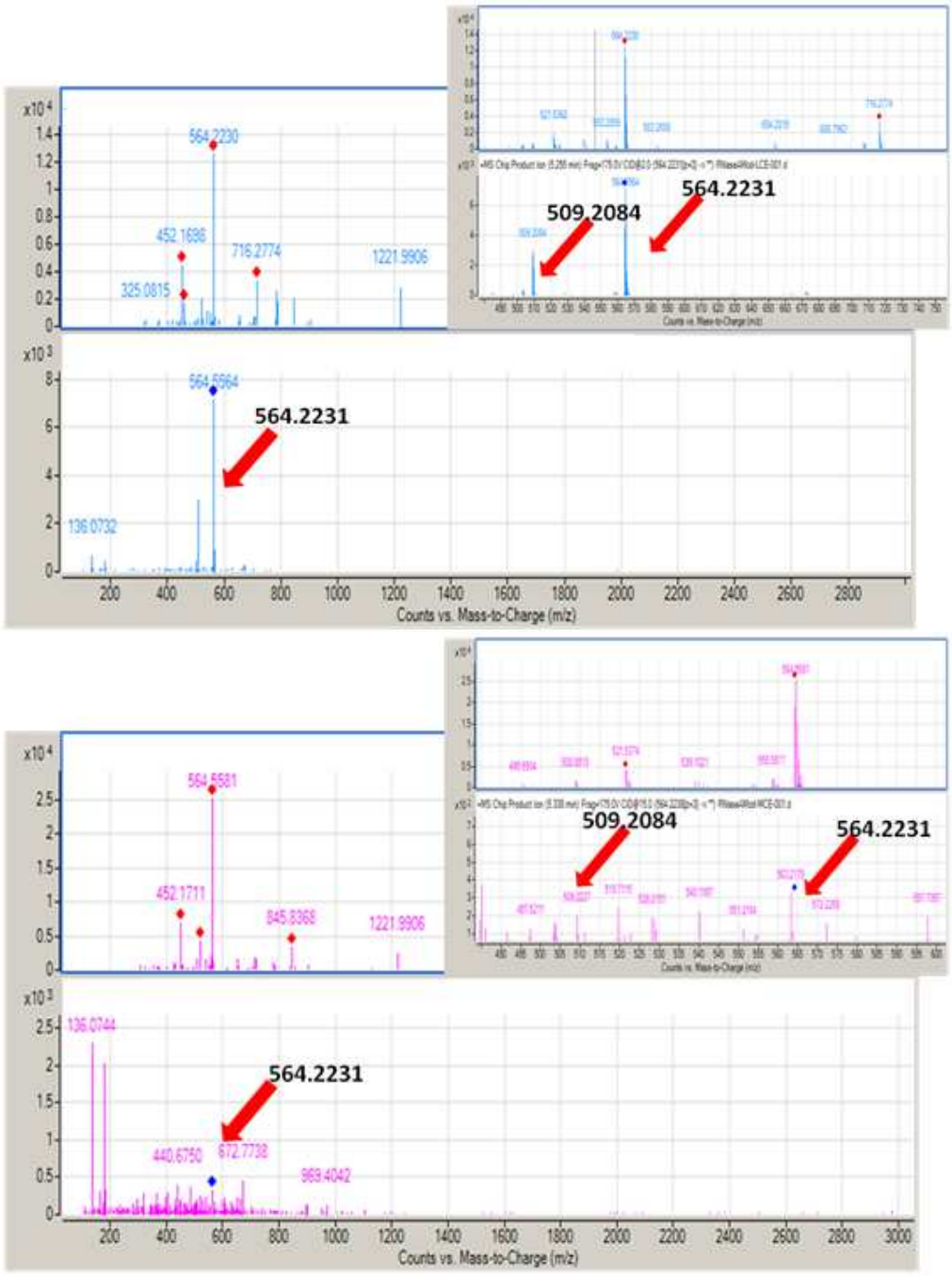

Figure 11: ESI results of peptide QHMDSSTSAASSSNY (QY) of "light" labeled RNaseA. (A)Modified QY peptide result with the collision energy setting at 2.0V/100Da. (B) Modified QY peptide result with the collision energy setting at 3.5V/100Da.

3.2.3 Results of "Light" and "Heavy" Isotopically Labeled Glucagon on MALDI-TOF

A 1μg/μL solution of Glucagon, containing aqueous 20% HOAc and 30% ACN, was modified with 1 M "light" or "heavy" PAB. The "light" and "heavy" labeled samples were then pooled together. MALDI analysis was performed when the derivatization reaction was initiated and completed after 24h (Figure 12).

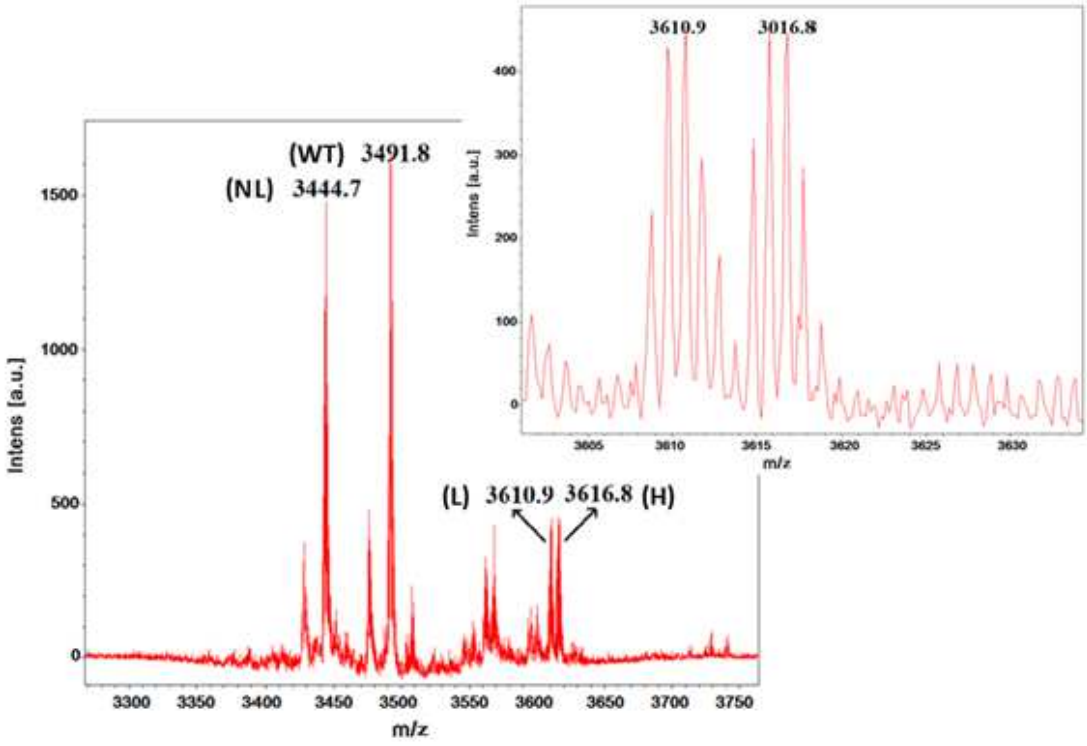

Figure 12: MALDI results of Glucagon 24h after modification. It is obtained via reflectron mode without calibration, thus the mass shifts from the accurate one a little bit. However, it won't affect the result since we only concern about the relative mass rather than the absolute mass. The inset is the amplifying spectrum at mass range of 3600Da-3635Da.

The mass of "light" and "heavy" phenacyl group (R=$CH_2COC_6H_5$ or R=$CH_2CO^{13}C_6H_5$) are 119.04Da and 125.05Da, respectively, and the mass of the expected

"light" and "heavy" NL ($C_9H_{10}SO$) are 166.05Da and 172.06Da, respectively. It should be noted that both the "light" and "heavy" labeled peptides produce the NL peaks with the same m/z since the differential parts are eliminated as the NL. For the mixture of "light" and "heavy" labeled Glucagon, a clear pair of peaks can be distinguished as the "light" labeled peptide peak at m/z=3610.9 and the "heavy" labeled peptide peak at m/z=3616.8, since they are 119.1Da and 125.0Da away from the wild-type peak at m/z=3491.8, respectively. The peak at m/z=3444.7 can also be distinguished as the NL peak, since it is 166.2Da and 172.1Da away from the "light" and "heavy" peaks, respectively. More importantly, it should be pointed out that the intensities of the "light" and "heavy" peaks are nearly the same as expected.

3.2.4 Results of "Light" and "Heavy" Isotopically Labeled Ribonuclease A on ESI-Qq-TOF Coupled with High-Performance Liquid Chromatography (HPLC)

A protease digested RNaseA sample was divided into two identical samples, each of which was isotopicallly labeled with "light" or "heavy" PAB. The "light" and "heavy" labeled samples were then pooled together and the mixture was desalted and analyzed by LC-MS/MS. Figure 13 depicts the mass spectrum and product ion mass spectrum obtained for a triply-charged Met peptide of the RNaseA mixture, at the collision energy setting of 2.0V/100Da (which is about one half of the collision energy setting, 3.5V/100Da, that is typically used for sequencing). The reason of employing this collision energy is based on the LC-MS/MS results of Substance P *(See Section 3.2.1)*. A

clear pair of peaks can be observed for the "light" labeled peptide peak at m/z=564.2289 and the "heavy" labeled peptide peak at m/z=566.2349. A peak at m/z=508.8803 can also be observed, which is consistent with that expected for the NL.

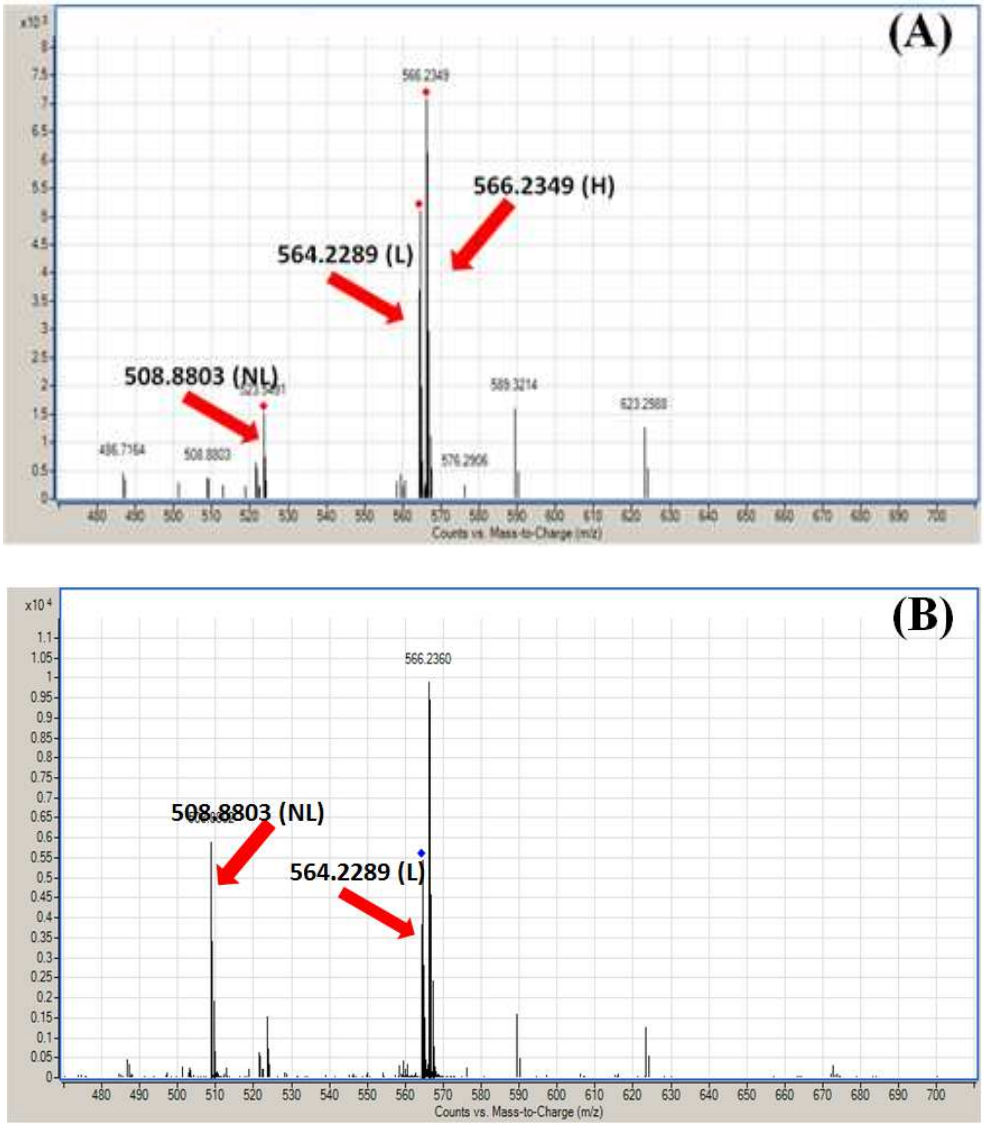

Figure 13: LC-MS/MS results of peptide QHMDSSTSAASSSNY (QY) of RNaseA mixture when the collision energy setting was 2.0V/100Da. (A) Mass spectrum. (B) Product ion mass spectrum of "light" and "heavy" labeled triply-charged peptide QY at m/z=564.2289 and m/z=566.2349.

Moreover, intensive and sharp peaks can be achieved when ion chromatograms were extracted in MS level with m/z=564.2349 and m/z=566.2349, both at retention time of 5.073min (Figure 14). In addition, the areas under the curves were acquired when the MS level-EIC with m/z=564.2349 and m/z=566.2349 were integrated, and the ratio of the areas was close to one (L/H=0.9429) as expected. Nevertheless, peptide identification was frustrating: many peptides can be identified for RNaseA with Agilent's Spectrum Mill MS Proteomics Workbench software but few of them were Met peptides, even though Met peptides absolutely existed according to the spectrum. Such issue with identification indicates current search engine algorithms cannot identify either modified or NL type peptides since they produce variable b/y ions when they fragment, though these variable but expectable b/y ions can be seen in the spectrum.

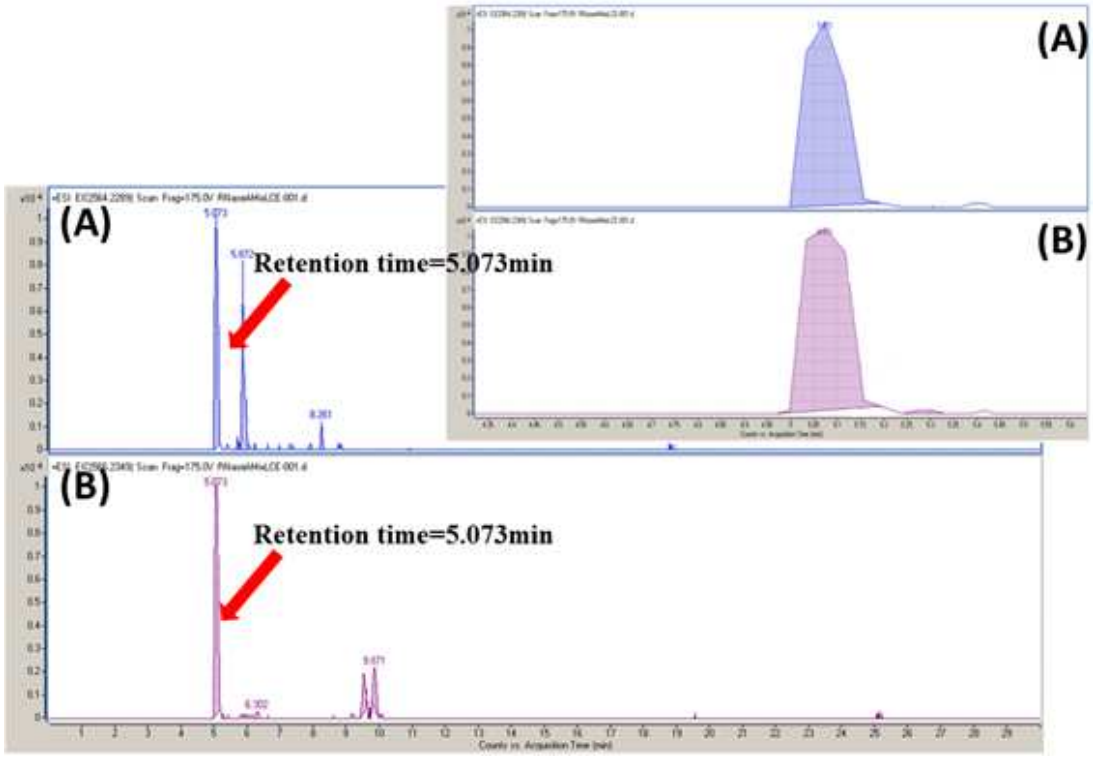

Figure 14: Extracted ion chromatogram (EIC) in MS level of RNaseA mixture. (A) EIC of peptide ion with m/z=564.2289. (B) EIC of peptide ion with m/z=566.2349. The inset is the amplifying EIC at time range of 4.3min-5.6min.

3.2.5 Results of "Light" and "Heavy" Isotopically Labeled Yeast Cell Lysate on ESI-Qq-TOF Coupled with HPLC

It is stated above that peptide identification with Spectrum Mill software is challenging since either modified or NL type peptides will produce variable b/y ions when they fragment. However, Met peptides can still be identified and even quantified by acquiring a precursor neutral loss chromatogram (pNLC). The pNLC is the chromatogram of product ions coming from precursor ions which yield NL with certain mass during Collision-Induced Dissociation (CID).

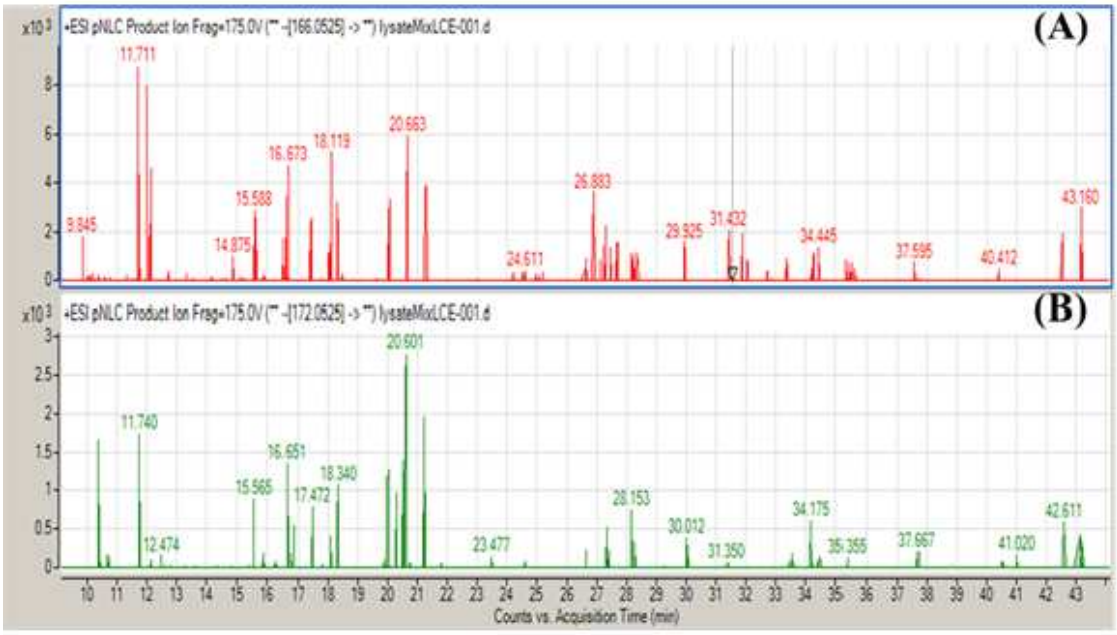

Figure 15: The amplifying pNLC in MS/MS level at time range of 9min-43min, with the NL mass of 166.05 (A) and 172.06 (B), respectively.

A yeast cell lysate was digested with trypsin and then divided into two identical samples, each of which was isotopically labeled with "light" or "heavy" PAB. The two samples were then pooled together and the mixture was desalted using C_{18} resin for LC-MS/MS analysis with 2.0V/100Da collision energy setting. Figure 15 shows the pNLC in MS/MS level with the mass of NL 166.05 and 172.06, respectively. Peptides with peaks existing in both of the pNLC can be identified as Met peptides. In this analysis, 18 Met peptides could be identified using this strategy. Subsequently, the ion chromatograms in MS level with m/z of "light" and "heavy" labeled peptides were extracted and integrated. The areas under the curves as well as the ratio of them were shown in Table

3. The average of these ratios for the 18 identified Met peptides was 1.1 with standard deviation of 0.1. This suggests that it can be used to quantify peptides. Further identification of these peptides can be achieved through LC-MS/MS for the same but unmodified yeast cell lysate at corresponding retention time.

Table 3: The areas under the curves of EIC in MS level with m/z of "light" and "heavy" labeled Met peptides, as well as the area ratio L/H.

m/z (L)	m/z (H)	z	Area (L)	Are (H)	Area Ratio
477.2395	479.2453	3	65267	73040	0.893579
744.376	747.386	2	32758	28699	1.141433
511.617	513.6234	3	289090	265765	1.087766
522.277	524.2811	3	75726	64559	1.172974
552.611	554.617	3	37489	41164	0.910723
556.9498	558.9564	3	37415	32664	1.145451
632.6756	634.6791	3	140781	120531	1.168007
702.8726	705.8806	2	19015	15654	1.214706
490.5029	492.0011	4	166149	180764	0.919149
655.3259	657.3371	3	167831	167377	1.002712
688.3661	690.3746	3	82471	73392	1.123706
535.038	536.542	4	79038	72996	1.082772
562.54	564.0457	4	59594	53242	1.119304
596.2988	597.8073	4	85973	75001	1.146291
596.5551	598.0595	4	80365	75656	1.062242
608.0511	609.5551	4	9583	8406	1.140019
637.8568	639.3512	4	96987	94547	1.025807
674.0962	675.6017	4	42201	41636	1.01357
				Average	**1.076123**
				Stdev	**0.096027**

4. RESULTS AND DISCUSSION FOR METHOD APPLICATION

4.1 Exploration of ATP-catalyzed Metabolism within Yeast Cells

The ATP binding properties of the proteins in a yeast cell lysate were analyzed using the SPROX-iTRAQ protocol. The ligand in the ATP binding study was AMP-PNP, a non-hydrolyzable ATP mimic. Also, Mg^{2+} was added since it is necessary for proteins to bind with ATP. The experiment enabled a total of 735 unique yeast proteins and 978 unique yeast proteins to be identified for the (+) and (-) sample, respectively. Among them, 418 unique proteins were identified via a Met-containing peptide filtered in the Excel file, with high summed iTRAQ intensity values (typically summed values >1000) as well as high and medium identification score, for the (+) sample and 414 unique proteins for the (-) sample. There were 610 unique Met-containing peptides mapped 294 unique proteins that are common to both the (-) and (+) samples. The distribution of the N2-normalized values at the low and high denaturant concentrations for the unoxidized Met-containing peptides that are common to both the (-) and (+) samples was examined and where the distributions cross was decided as the "cut-off" value of a theoretical curve, which was 0.9 (typically around 1.0) in this experiment (Figure 5). It should be noted that the distribution of N2-normalized values at the high denaturant concentration is 0.7 (typically centered around 0.5) and the distribution of N2-normalized values at the lowest denaturant concentration is 1.1 (typically centered around 1.5). This means the amplitude of SPROX data sets in this experiment is smaller

than usual. Through differences analysis, there were 285 Met peptides mapped 170 proteins were identified as potential hits. Then, a visual inspection was generated for these potential hits to determine which peptides have significant transition midpoint differences (>1 M for urea) in the (-) and (+) samples and revealed three peptides from three proteins with transition midpoint shifts of >1.0 M urea in the presence of AMP-PNP. All of these three proteins have known ATP binding interactions based on annotations (i.e., GO TERM = ATP binding) in the yeast genome database, which are ADEnine requiring (YGR204W), URAcil requiring (YJL130C), Yeast Elongation Factor (YLR249W). The SPROX data sets of them are shown below in Figure 16.

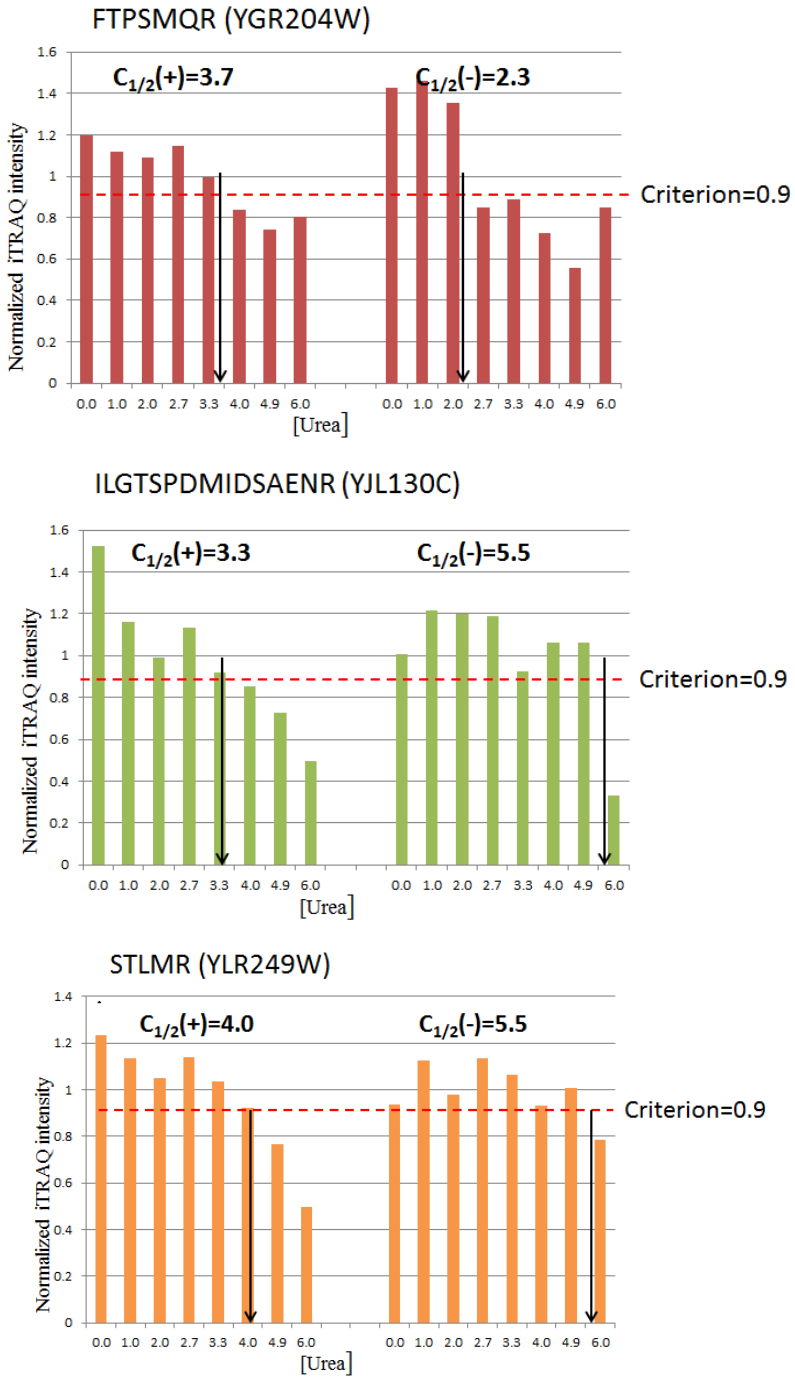

Figure 16: SPROX data sets for ADEnine requiring (YGR204W), URAcil requiring (YJL130C) and Yeast Elongation Factor (YLR249W)

4.2 Identification of Iron Chelators Protecting Mechanism in Mammalian Cells

The samples were analyzed using the SPROX-iTRAQ protocol. In this study, ARPE-19 cell lines were used and there are two chelators we are interested in, HAPI and Exjade. The experiment enabled a total of 884 unique mammalian proteins, 916 unique mammalian proteins and 726 unique mammalian proteins to be identified for the with ligand Exjade (+E) sample, with ligand HAPI (+H) sample and without ligand (-) sample, respectively. Among them, 752 unique proteins were identified via a Met-containing peptide filtered in the Excel file for the (+E) sample, 789 unique proteins for (+H) sample, and 648 unique proteins for the (-) sample. However, there were only 48 unique Met-containing peptides mapped 37 unique proteins that are common to both the (-) and (+E) samples and 38 unique Met-containing peptides mapped 26 unique proteins that are common to both the (-) and (+H) samples (Table 4).

Table 4: Results summary for the experiment to identify the protein targets of iron chelator in mammalian cells

	Without Ligand Peptide (Protein)	*With Exjade Peptide (Protein)*	*With HAPI Peptide (Protein)*
Int>1000	870 (648)	1019 (752)	1115 (789)
Met Peptide	224 (170)	264 (200)	281 (221)
Matched Met	——	48 (37)	38 (26)

The distribution of the N2-normalized values at the low and high denaturant concentrations for the unoxidized Met-containing peptides that are common to both the with and without ligand samples was examined and where the distributions cross was

decided as the “cut-off” value of a theoretical curve; however, this approximate transition midpoint cannot be determined in this experiment due to the limited amount of identified unoxidized Met-containing peptides. Through differences, there were 17 Met peptides mapped 14 proteins were identified as potential hits for ligand Exjade and six Met peptides mapped five proteins were identified as potential hits for ligand HAPI. Then a visual inspection was generated for these potential hits to determine which peptides have significant transition midpoint differences (>0.5 M for GdmCl) in the with and without ligand samples. It revealed the peptide MPEIR (from protein V-type proton ATPase subunit E2) has transition midpoint shifts of >0.5 M GdmCl in the presence of Exjade and the peptide MALDIEIATYR (from an unnamed protein) has transition midpoint shifts of >0.5 M GdmCl in the presence of HAPI. SPROX data sets of them are shown below in Figure 17.

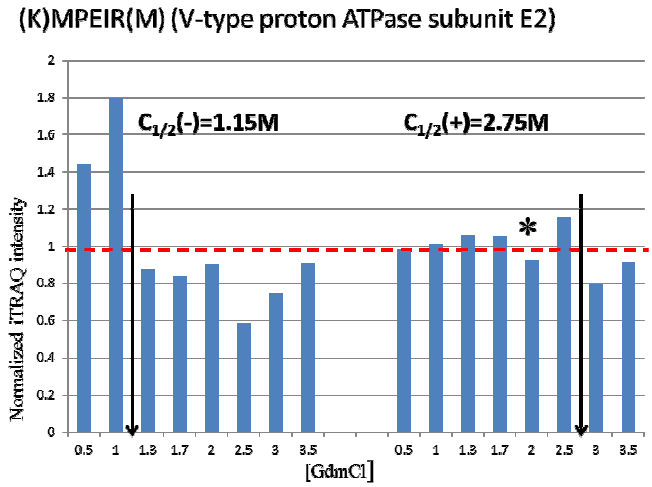

(A)

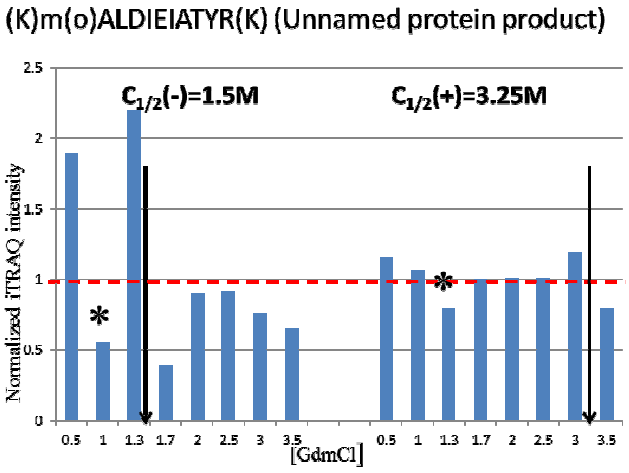

(B)

Figure 17: SPROX data sets of potential hits for (A) Exjade (B) HAPI. Even though the distributions were unsatisfying, the results of abundant previous work show the "cut-off" value is always around 1, which is the cut-off value used in this experiment. An asterisk represents an outlying data point.

5. CONCLUSION

5.1 Method Development

In the gel-phase fractionation studies, the comparison between the results of in-gel digestion and in-solution digestion shows gel electrophoresis can help obtain complementary peptide identification and thus increase the proteome coverage. The results of iTRAQ-labeling in-gel digested proteins indicate satisfying reproducibility as well as maintainable quantitation capabilities.

In the gas-phase fractionation studies, both MALDI-TOF and ESI-Qq-TOF results of model systems show the derivatization reaction is effective, though not complete. The incomplete modification will not impair the quantitation capabilities since the quantitation is based on the relative abundances of "light" and "heavy" labeled peptides. However, a more complete modification will enhance the selectivity for detection of Met-containing peptides. Moreover, the high-quality area ratios of "light" and "heavy" labeled peptide peaks indicate the satisfying quantitation capabilities, and comparing to that of iTRAQ-labeling (~25%)19, the quantitation capabilities are significantly improved (~10%). In addition, Met-containing peptides can be distinguished from a yeast cell lysate through the pNLC, even though it is difficult to identify these peptides with Spectrum Mill software. This provides the convincing evidence that gas-phase fragmentation on a triple quadrupole in the neutral loss scan mode will increase selectivity for detection of Met-containing peptides.

These promising initial results reveal both fractionation strategies interfaced with SPROX could facilitate increasing the proteome coverage and Met selectivity as well as improving quantitation capabilities for studies in protein-ligand binding interactions. Consequently, both fractionation strategies have the potential for us to better study thermodynamic stability of proteins and protein-ligand interactions on proteomic scale, and most importantly, to gain more information about biological processes within the cell as well as drug design.

5.2 Method Application

The well-established shotgun proteomic technique incorporating SPROX with isobaric mass tags (SPROX-iTRAQ) was used in a protein-ligand binding study designed to identify the protein targets in a yeast cell lysate of AMP-PNP, a non-hydrolyzable ATP mimic. Three proteins were identified as hits in the assay and all of them have known ATP binding interactions in the yeast genome database, which are ADEnine requiring, URAcil requiring and Yeast Elongation Factor. However, it is clear that a great amount of ATP binding protein targets in the yeast genome database cannot be identified as hits. This yields a very high false negative rate of the assay. Besides the limitation of SPROX-iTRAQ technique, which is only proteins identified with a Met-containing peptide can be included in the assay, another reason is that the amplitude of SPROX data sets in this experiment is relatively smaller than usual, which makes the visual inspection hard to be performed.

Application of SPROX-iTRAQ technique to the investigation of the protein targets in a mammalian cell lysate that bind iron chelators identified one potential target for each chelator, V-type proton ATPase subunit E2 for Exjade and an unnamed protein for HAPI. Despite the decent amounts for both total identified proteins and Met-containing proteins with high summed iTRAQ intensity values, the number of proteins that are common to both the with and without ligand samples is very low. It is no wonder that few protein targets were identified as hits in the assay. Further investigation needs to be implemented.

References

1. Miller, K.R. and D.P. Cistola, Titration calorimetry as a binding assay for lipid-binding proteins. Mol Cell Biochem, 1993. 123(1-2): p. 29-37.

2. Burova, T.V., et al., Conformational stability and binding properties of porcine odorant binding protein. Biochemistry, 1999. 38(45): p. 15043-51.

3. Pedigo, S. and M.A. Shea, Discontinuous equilibrium titrations of cooperative calcium binding to calmodulin monitored by 1-D 1H-nuclear magnetic resonance spectroscopy. Biochemistry, 1995. 34(33): p. 10676-89.

4. Hill, J.J. and C.A. Royer, Fluorescence approaches to study of protein-nucleic acid complexation. Methods Enzymol, 1997. 278: p. 390-416.

5. Giot, L., et al., A protein interaction map of Drosophila melanogaster. Science, 2003. 302(5651): p. 1727-36.

6. Li, S., et al., A map of the interactome network of the metazoan C. elegans. Science, 2004. 303(5657): p. 540-3.

7. Rual, J.F., et al., Towards a proteome-scale map of the human protein-protein interaction network. Nature, 2005. 437(7062): p. 1173-8.

8. Uetz, P., et al., A comprehensive analysis of protein-protein interactions in Saccharomyces cerevisiae. Nature, 2000. 403(6770): p. 623-7.

9. Ho, Y., et al., Systematic identification of protein complexes in Saccharomyces cerevisiae by mass spectrometry. Nature, 2002. 415(6868): p. 180-3.

10. Gavin, A.C., et al., Functional organization of the yeast proteome by systematic analysis of protein complexes. Nature, 2002. 415(6868): p. 141-7.

11. Graumann, J., et al., Applicability of tandem affinity purification MudPIT to pathway proteomics in yeast. Mol Cell Proteomics, 2004. 3(3): p. 226-37.

12. Ghaemmaghami, S., M.C. Fitzgerald, and T.G. Oas, A quantitative, high-throughput screen for protein stability. Proc Natl Acad Sci U S A, 2000. 97(15): p. 8296-301.

13. Powell, K.D., et al., A general mass spectrometry-based assay for the quantitation of protein-ligand binding interactions in solution. J Am Chem Soc, 2002. 124(35): p. 10256-7.

14. Zhu, M.M., et al., Quantification of protein-ligand interactions by mass spectrometry, titration, and H/D exchange: PLIMSTEX. J Am Chem Soc, 2003. 125(18): p. 5252-3.

15. Charvatova, O., et al., Quantifying protein interface footprinting by hydroxyl radical oxidation and molecular dynamics simulation: application to galectin-1. J Am Soc Mass Spectrom, 2008. 19(11): p. 1692-705.

16. Hopper, E.D., et al., Hydrogen/deuterium exchange- and protease digestion-based screening assay for protein-ligand binding detection. Anal Chem, 2009. 81(16): p. 6860-7.

17. Dearmond, P.D., et al., Thermodynamic analysis of protein-ligand interactions in complex biological mixtures using a shotgun proteomics approach. J Proteome Res, 2011. 10(11): p. 4948-58.

18. West, G.M., L. Tang, and M.C. Fitzgerald, Thermodynamic analysis of protein stability and ligand binding using a chemical modification- and mass spectrometry-based strategy. Anal Chem, 2008. 80(11): p. 4175-85.

19. West, G.M., et al., Quantitative proteomics approach for identifying protein-drug interactions in complex mixtures using protein stability measurements. Proc Natl Acad Sci U S A, 2010. 107(20): p. 9078-82.

20. Havlis, J. and A. Shevchenko, Absolute quantification of proteins in solutions and in polyacrylamide gels by mass spectrometry. Anal Chem, 2004. 76(11): p. 3029-36.

21. Havlis, J., et al., Fast-response proteomics by accelerated in-gel digestion of proteins. Anal Chem, 2003. 75(6): p. 1300-6.

22. Schmidt, C. and H. Urlaub, iTRAQ-labeling of in-gel digested proteins for relative quantification. Methods Mol Biol, 2009. 564: p. 207-26.

23. Shevchenko, A., et al., In-gel digestion for mass spectrometric characterization of proteins and proteomes. Nat Protoc, 2006. 1(6): p. 2856-60.

24. Amunugama, M., K.D. Roberts, and G.E. Reid, Mechanisms for the selective gas-phase fragmentation reactions of methionine side chain fixed charge sulfonium ion containing peptides. J Am Soc Mass Spectrom, 2006. 17(12): p. 1631-42.

25. Reid, G.E., et al., Selective identification and quantitative analysis of methionine containing peptides by charge derivatization and tandem mass spectrometry. J Am Soc Mass Spectrom, 2005. 16(7): p. 1131-50.

26. Roberts, K.D. and G.E. Reid, Leaving group effects on the selectivity of the gas-phase fragmentation reactions of side chain fixed-charge-containing peptide ions. J Mass Spectrom, 2007. 42(2): p. 187-98.

27. Froelich, J.M., S. Kaplinghat, and G.E. Reid, Automated neutral loss and data dependent energy resolved "pseudo MS3" for the targeted identification, characterization and quantitative analysis of methionine- containing peptides. Eur J Mass Spectrom (Chichester, Eng), 2008. 14(4): p. 219-29.

28. Hardie, D.G. and S.A. Hawley, AMP-activated protein kinase: the energy charge hypothesis revisited. Bioessays, 2001. 23(12): p. 1112-9.

29. Knowles, J.R., Enzyme-catalyzed phosphoryl transfer reactions. Annu Rev Biochem, 1980. 49: p. 877-919.

30. Goldberg, A.L., The mechanism and functions of ATP-dependent proteases in bacterial and animal cells. Eur J Biochem, 1992. 203(1-2): p. 9-23.

31. Gottesman, S. and M.R. Maurizi, Regulation by proteolysis: energy-dependent proteases and their targets. Microbiol Rev, 1992. 56(4): p. 592-621.

32. Goldberg, A.L., ATP-dependent proteases in prokaryotic and eukaryotic cells. Semin Cell Biol, 1990. 1(6): p. 423-32.

33. Hlavacek, O. and L. Vachova, ATP-dependent proteinases in bacteria. Folia Microbiol (Praha), 2002. 47(3): p. 203-12.

34. Rotanova, T.V., [Energy-dependent selective intracellular proteolysis. Structure, active sites and specificity of ATP-dependent proteinases]. Vopr Med Khim, 2001. 47(1): p. 3-19.

35. Voellmy, R.W. and A.L. Goldberg, ATP-stimulated endoprotease is associated with the cell membrane of E. coli. Nature, 1981. 290(5805): p. 419-21.

36. Waxman, L. and A.L. Goldberg, Selectivity of intracellular proteolysis: protein substrates activate the ATP-dependent protease (La). Science, 1986. 232(4749): p. 500-3.

37. Rohrwild, M., et al., HslV-HslU: A novel ATP-dependent protease complex in Escherichia coli related to the eukaryotic proteasome. Proc Natl Acad Sci U S A, 1996. 93(12): p. 5808-13.

38. Richardson, D.R., et al., Cancer cell iron metabolism and the development of potent iron chelators as anti-tumour agents. Biochim Biophys Acta, 2009. 1790(7): p. 702-17.

39. Glickstein, H., et al., Intracellular labile iron pools as direct targets of iron chelators: a fluorescence study of chelator action in living cells. Blood, 2005. 106(9): p. 3242-50.

40. Neufeld, E.J., Update on iron chelators in thalassemia. Hematology Am Soc Hematol Educ Program, 2010. 2010: p. 451-5.

41. Ward, R., An update on disordered iron metabolism and iron overload. Hematology, 2010. 15(5): p. 311-7.

42. Boddaert, N., et al., Selective iron chelation in Friedreich ataxia: biologic and clinical implications. Blood, 2007. 110(1): p. 401-8.

43. Hadziahmetovic, M., et al., The oral iron chelator deferiprone protects against iron overload-induced retinal degeneration. Invest Ophthalmol Vis Sci, 2011. 52(2): p. 959-68.

44. Hruskova, K., et al., Synthesis and initial in vitro evaluations of novel antioxidant aroylhydrazone iron chelators with increased stability against plasma hydrolysis. Chem Res Toxicol, 2011. 24(3): p. 290-302.

45. Kalinowski, D.S. and D.R. Richardson, The evolution of iron chelators for the treatment of iron overload disease and cancer. Pharmacol Rev, 2005. 57(4): p. 547-83.

46. Kielar, F., et al., Prochelator BHAPI protects cells against paraquat-induced damage by ROS-triggered iron chelation. Metallomics, 2012. 4(9): p. 899-909.

47. Perez, L.R. and K.J. Franz, Minding metals: tailoring multifunctional chelating agents for neurodegenerative disease. Dalton Trans, 2010. 39(9): p. 2177-87.

48. Sterba, M., et al., Iron chelation-afforded cardioprotection against chronic anthracycline cardiotoxicity: a study of salicylaldehyde isonicotinoyl hydrazone (SIH). Toxicology, 2007. 235(3): p. 150-66.

49. Zhou, T., et al., Design of iron chelators with therapeutic application. Dalton Trans, 2012. 41(21): p. 6371-89.

50. Hasinoff, B.B., D. Patel, and X. Wu, The oral iron chelator ICL670A (deferasirox) does not protect myocytes against doxorubicin. Free Radic Biol Med, 2003. 35(11): p. 1469-79.

51. Kidson-Gerber, G. and R. Lindeman, Adherence to desferrioxamine and deferiprone and the impact of deferiprone co-prescription in thalassaemia major patients. Does the addition of deferiprone improve adherence? Br J Haematol, 2008. 142(4): p. 679-80.

52. Simunek, T., et al., Anthracycline toxicity to cardiomyocytes or cancer cells is differently affected by iron chelation with salicylaldehyde isonicotinoyl hydrazone. Br J Pharmacol, 2008. 155(1): p. 138-48.

53. Bendova, P., et al., Comparison of clinically used and experimental iron chelators for protection against oxidative stress-induced cellular injury. Chem Res Toxicol, 2010. 23(6): p. 1105-14.

54. Charkoudian, L.K., et al., Iron prochelator BSIH protects retinal pigment epithelial cells against cell death induced by hydrogen peroxide. J Inorg Biochem, 2008. 102(12): p. 2130-5.

55. Klimtova, I., et al., A study of potential toxic effects after repeated 10-week administration of a new iron chelator--salicylaldehyde isonicotinoyl hydrazone (SIH) to rabbits. Acta Medica (Hradec Kralove), 2003. 46(4): p. 163-70.

56. Simunek, T., et al., SIH--a novel lipophilic iron chelator--protects H9c2 cardiomyoblasts from oxidative stress-induced mitochondrial injury and cell death. J Mol Cell Cardiol, 2005. 39(2): p. 345-54.

57. Haskova, P., et al., Comparison of various iron chelators used in clinical practice as protecting agents against catecholamine-induced oxidative injury and cardiotoxicity. Toxicology, 2011. 289(2-3): p. 122-31.

58. Strickland, E.C., et al., Thermodynamic analysis of protein-ligand binding interactions in complex biological mixtures using the stability of proteins from rates of oxidation. Nat Protoc, 2013. 8(1): p. 148-61.